Trapping and excitation of modes in the magnetotail

Katharine J. Mills and Andrew N. Wright[a)]
Mathematical Institute, University of St. Andrews, St. Andrews, Fife, Scotland, KY16 9SS

(Received 3 September 1999; accepted 22 December 1999)

A slab model of the magnetotail lobes is studied, and the trapping and excitation of fast magnetoacoustic modes is considered. The tail lobe is taken to be uniform with the magnetic-field stretching parallel to the flow in the magnetosheath. The modes are assumed to be trapped between free magnetopause boundaries. The ideal magnetohydrodynamic (MHD) equations are used to study the effects of linear perturbations to this equilibrium state. It is found that the plasma parameters in this region mean that fast magnetoacoustic waves are unlikely to be Kelvin–Helmholtz (KH) unstable for realistic flow speeds, and in fact these modes are likely to be leaky, losing energy across the magnetopause boundary. However, the decay rates of modes propagating both with and against the magnetosheath flow are found to be small for reasonable plasma parameters and this boundary may be reasonably assumed to be reflecting for the purposes of wave guide theory. Slow modes are found to have very small growth rates and since in the magnetotail lobes the plasma beta is very low, they are not expected to be important. © *2000 American Institute of Physics.*
[S1070-664X(00)02104-2]

I. INTRODUCTION

In this paper we examine the trapping and driving of modes in the magnetotail by the shear flow in the magnetosheath. In the magnetotail the magnetic-field lines are stretched out parallel to the flow in the magnetosheath (see Fig. 1). The fact that the magnetosphere has a long tail has been known since the proposal of the open magnetosphere model by Dungey (1961).[1] Dungey (1965)[2] calculated the length of the magnetotail using the fact that reconnected field lines are connected to the Earth via the polar caps. Knowing the electric and magnetic-field strengths at the caps, the speed at which a field line would move across the cap was calculated and thus the time taken for a field line to convect from the reconnection point at the nose of the magnetosphere to the point at which the lines reconnect in the tail could be calculated. Multiplying this time by the solar wind speed, Dungey obtained a value of about $1000\,R_E$ for the length of the magnetotail. Magnetometer data show observations of oscillations with frequencies of the order of millihertz and lower [Herron (1967)[3]] and eigenfrequencies of the right order have been found by McClay and Radoski (1967)[4] using a cylindrical magnetotail (the ''theta'' model). The magnetic field in the theta model was taken to be uniform in the top and bottom of the wave guide, but with a reversal of direction across the middle. Models including the plasma sheet were also developed [Siscoe (1969);[5] McKenzie (1970b)[6]].

More recently work has included the behavior of waves in the high-density plasma/current sheet at the center of the magnetotail [e.g., Seboldt (1990);[7] Liu *et al.* (1995)[8]]. It has been shown that waves may be trapped in the low Alfvén speed region at the center of a current sheet [Edwin *et al.* (1986);[9] Smith *et al.* (1997)[10]].

Pu and Kivelson (1983)[11] modeled the surface waves at the magnetopause for a magnetotail like geometry. They considered an infinite uniform region on either side of the magnetopause with both the magnetic fields in the magnetosphere and magnetosheath being parallel to the flow in the magnetosheath. They showed that the flow speed at the onset of the instability of the fast surface mode varies little with the angle of propagation and was close to the onset of the instability for an incompressible plasma.

Elphinstone *et al.* (1995)[12] observed fast waves traveling towards the Earth using the IMP 8 satellite. These modes were linked with a source $30\,R_E$ down tail and indicated that the magnetotail could act like a wave guide for these modes. Allan and Wright (1998)[13] showed that the nonuniform nature of the magnetic field allows these fast wave guide modes to couple to Alfvén waves in the outer tail which will travel earthward faster than the fast modes that are confined to the middle of the tail.

In this paper we study the nature of the magnetospheric boundary in the tail, and thus examine the ability of the magnetotail to trap and excite modes between the northern and southern magnetopauses for a slab model of the magnetotail. Our calculation is best thought of as an extension of the models which have a single magnetopause separating two semi-infinite media [e.g., McKenzie (1970a);[14] Pu and Kivelson (1983)[11]]. Our calculation includes a finite size magnetotail wave guide, in contrast to the semi-infinite tail lobe of these studies. We are primarily concerned with the effect of a finite width tail, and so take a uniform tail in this preliminary investigation, rather than including a realistic plasma sheet, lobe and mantle structure. We are able to consider both symmetric or antisymmetric modes, and in this paper focus upon those with a node of normal plasma displacement at the tail center as these should be relevant to studying sub-storm-related phenomena. It was shown that the trapping and excitation of modes in the magnetospheric flanks is determined by the local properties of the plasmas

[a)]Electronic mail: andy@dcs.st-and.ac.uk

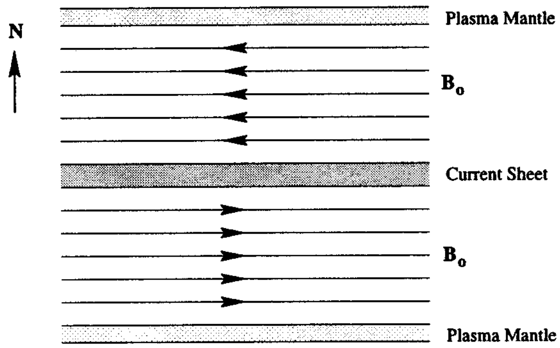

FIG. 1. A schematic diagram of the geometry in the magnetotail. We have taken a cut from North to South and the Earth is to the left in this picture.

either sides of the magnetopause [Mills *et al.* (1999);[15] Mills and Wright (1999)[16]] which is true in this case also, and so we model our tail as effectively and extended lobe.

The structure of this paper is as follows: In Sec. II we set up our model, the results for slow modes are summarized in Sec. III, and the results for fast modes are presented in Sec. IV. Finally, in Sec. V we summarize our results and discuss the consequences for the magnetotail.

II. MODEL AND EQUATIONS

We consider a straight bounded model of the magnetotail lobe with a free boundary connecting it to the magnetosheath so that energy from the magnetosheath flow may pass into the magnetotail and drive unstable modes, while leaky modes may lose energy from the tail into the magnetosheath. The magnetotail is taken to have a uniform straight equilibrium magnetic-field $\mathbf{B}$ in the y direction, and a nonzero plasma pressure, P_1, and density ρ_{o1} (see Fig. 2). The model magnetosheath has no equilibrium magnetic field, a finite plasma pressure, P_2, and density, ρ_{o2} and is taken to be flowing in the y direction with a uniform speed, v_o. Throughout this paper we will use quantities normalized to the equilibrium density and sound speed, c_{s2} in the magnetosheath and the depth of the tail lobe, d. Plasma pressure is normalized by the quantity ΓP_2, magnetic fields by $\sqrt{\Gamma P_2 \mu_o}$, where Γ is the ratio of specific heats, and time by d/c_{s2}.) Thus we take the magnetopause to be situated at $x=1$ and from here-on in, all quantities referred to will be taken to be in normalized units.

We add a small perturbation to each of our equilibrium quantities and normalize and Fourier analyze the ideal MHD equations to obtain our dispersion relation

$$\epsilon\left(\frac{\omega^2-k^2v_{a1}^2\cos^2\alpha}{m_1}\right)\left(\frac{\exp(im_1)+\exp(-im_1)}{\exp(im_1)-\exp(-im_1)}\right)-\frac{\omega'^2}{m_2}=0, \tag{1}$$

where ω is the frequency of the oscillations which we allow to be complex so that $\omega=\omega_r+i\omega_i$, $\mathbf{k}=(0,k_y,k_z)$ is the wave vector tangential to the magnetopause boundary, α is the angle between the wave vector and the equilibrium magnetic field, $\epsilon=\rho_{o1}/\rho_{o2}$ is the ratio of the inner and outer densities, and m_1 and m_2 are the wave numbers in the x direction in the magnetotail and magnetosheath, respectively. These wave numbers are defined as

$$m_1^2=\frac{(\omega^2-k^2c_f^2)(\omega^2-k^2c_{\rm slow}^2)}{(c_f^2+c_{\rm slow}^2)(\omega^2-k^2c_T^2)}, \tag{2}$$

$$m_2^2=\frac{\omega'^2-k^2c_{s2}^2}{c_{s2}^2}, \tag{3}$$

where c_f and $c_{\rm slow}$ are the fast and slow magnetoacoustic speeds in the magnetotail respectively, given by

$$c_{f/\rm slow}^2=\tfrac{1}{2}((v_{a1}^2+c_{s1}^2) +/-\sqrt{(v_{a1}^2+c_{s1}^2)^2-4v_{a1}^2c_{s1}^2\cos^2\alpha}), \tag{4}$$

with v_{a1} and c_{s1} defined as the sound and Alfvén speeds in the magnetotail, respectively. c_T is the tube speed along the wave vector defined by

$$c_T^2=\frac{c_f^2c_{\rm slow}^2}{c_f^2+c_{\rm slow}^2}=\frac{v_{a1}^2c_{s1}^2}{v_{a1}^2+c_{s1}^2}\cos^2\alpha, \tag{5}$$

and $\omega'=\omega-kv_o\cos\alpha$ is the Doppler-shifted frequency in the rest frame of the magnetosheath. When ω is purely real (i.e., the modes are stable) we may classify the modes as either body or surface modes. This is defined by the sign of m_1^2. If $m_1^2<0$ (so that $\omega/k<c_T$ or $c_{\rm slow}<\omega/k<c_f$) the modes are surface modes and have an evanescent character in the magnetotail lobe. The dispersion relation for stable surface modes may be written as

$$\tanh(n_1)=\frac{\epsilon}{c_{s2}}\frac{(\omega^2-k^2v_{a1}^2\cos^2\alpha)}{(\omega-kv_o\cos\alpha)^2}\sqrt{\frac{(c_{s2}^2-(\omega-kv_o\cos\alpha)^2)(c_f^2+c_{\rm slow}^2)(\omega^2-k^2c_T^2)}{(k^2c_f^2-\omega^2)(\omega^2-k^2c_{\rm slow}^2)}}, \tag{6}$$

where $n_1^2=-m_1^2$. When $m_1^2>0$ (so that $c_T<\omega/k<c_{\rm slow}$ or $\omega/k>c_f$) we find body modes, which have an oscillatory character in the magnetotail lobe. The dispersion relation for stable body modes may be written as

$$\tan(m_1)=\frac{\epsilon}{c_{s2}}\frac{(\omega^2-k^2v_{a1}^2\cos^2\alpha)}{(\omega-kv_o\cos\alpha)^2}\sqrt{\frac{(c_{s2}^2-(\omega-kv_o\cos\alpha)^2)(c_f^2+c_{\rm slow}^2)(\omega^2-k^2c_T^2)}{(\omega^2-k^2c_f^2)(\omega^2-k^2c_{\rm slow}^2)}}, \tag{7}$$

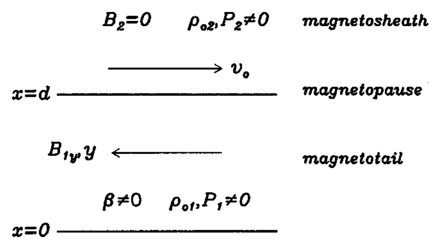

FIG. 2. A schematic representation of the northern half of our bounded magnetotail model.

When the modes are unstable ($\omega_i \neq 0$) the modes cannot be classified so neatly into body and surface modes. Indeed, in both the magnetotail and the magnetosheath, an unstable mode will have an oscillatory character with a growth or decay envelope. We will then be able to classify modes only by their dominant spatial behavior in the magnetotail.

We have assumed the normal plasma displacement is antisymmetric about $x=0$ and the boundary conditions at the magnetopause are the total pressure and displacement in the x direction are continuous. In the magnetosheath we use the condition that the x component of the group velocity in the magnetosheath plasma rest frame must be directed away from the magnetopause (it must be positive) which gives the condition that

$$\mathrm{Re}(\omega')\mathrm{Re}(m_2)+\mathrm{Im}(\omega')\mathrm{Im}(m_2)>0, \tag{8}$$

and when the modes are stable, we require the modes to decay into the magnetosheath so that

$$\mathrm{Im}(m_2)>0. \tag{9}$$

Although the group velocity of the waves is a well-defined and meaningful quantity for real ω' and m_2, when these quantities are complex it is not so obvious that the above boundary conditions are appropriate. We can convince ourselves of their correctness by other considerations. For example, in the magnetosheath rest frame, we could require that the time-averaged energy flux of the wave be directed away from the magnetopause. Alternatively, we could consider an initial-value problem formulation in terms of a Fourier–Laplace integral. If the perturbation is to vanish at infinity then roots on the ''physical'' Riemann sheet [i.e., with $\mathrm{Im}(\omega')>0$] must have $\mathrm{Im}(m_2)>0$. Similarly, roots on the ''unphysical'' Riemann sheet [i.e., with $\mathrm{Im}(\omega')<0$] must have $\mathrm{Im}(m_2)<0$. These requirements are equivalent to those stated above. Such boundary conditions were used by Mann *et al.* (1999)[17] and Mills *et al.* (1999)[15] who also showed that stable modes may only exist if $m_2^2<0$ so that m_2 is purely imaginary. From Eq. (3) this gives a necessary condition for the existence of stable or trapped modes, i.e.,

$$v_o \cos\alpha - c_{s2} < v_{ph} < v_o \cos\alpha + c_{s2}. \tag{10}$$

We may further classify these modes as either fast (having $\omega_r/k>c_{\mathrm{slow}}$) or slow (having $\omega_r/k<c_{\mathrm{slow}}$).

Figure 3 shows the regions of $v_{ph}-\alpha$ space for which stable modes may exist as the region with negatively sloped shading, and the regions for which we would expect stable modes to be oscillatory in the magnetosphere (we expect to find body modes) as regions with positively sloped shading.

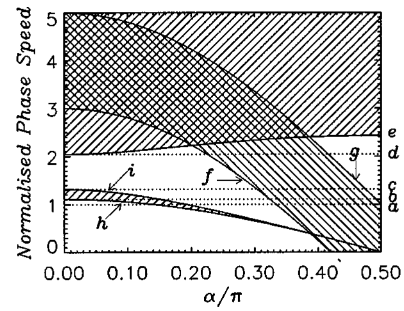

FIG. 3. The variation of the regions of phase speed (given in units of c_{s2}) where different mode types may exist with propagation angle α. Of the dotted lines, a is the magnetosheath sound speed (c_{s2}), b is the tube speed [$c_T(\alpha=0)$] in the magnetosphere when $\alpha=0$, c is the sound speed in the magnetosphere (c_{s1}) and d is the Alfvén speed in the magnetosphere (v_{a1}). Of the solid curves, f is the lower cutoff for stable modes ($v_{ph}=v_o\cos\alpha - c_{s2}$), g is the corresponding upper cutoff ($v_{ph}=v_o\cos\alpha+c_{s2}$), the fast speed is given by curve g while the curves of the slow speed, c_{slow} and tube speed, c_T are indicated by the arrows i and h, respectively. Here as in most of the following diagrams $\beta=0.5$, $\Gamma=5/3$, and $\epsilon=0.192$. We have also taken $v_o=4.0$.

The unshaded regions are those where we would expect to find modes that are evanescent in the magnetosphere (surface modes) if the modes were stable. The overlap of the shaded regions indicates the regions of parameter space in which we would expect to see stable body modes and the overlap between the region where stable modes may exist and the unshaded regions show where we would expect to find stable surface modes. In this figure we have taken $\beta=0.5$, $\epsilon=\rho_1/\rho_2=0.192$ and $v_o=4$.

Measurements of magnetopause crossings in the tail show that the density ratio between the magnetosphere and magnetosheath can lie anywhere within the range $0.01<\epsilon<0.2$. We have chosen a value close to the upper end of this range as this allows us to see unstable modes for lower flow speeds. Figure 4 shows the dependence of the characteristic wave speeds in the magnetosphere on the density ratio ϵ. We can see that, when the density range is lowest, the fast, slow and tube speeds become much larger than the sound speed in the magnetosheath and since the onset of instability for the fast body modes (for example) requires that

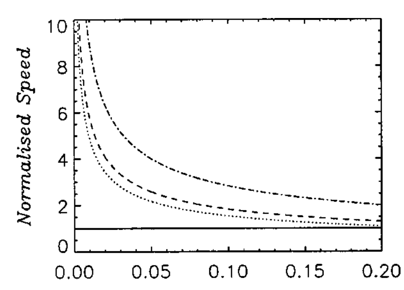

FIG. 4. The variation of the characteristic wave speeds in the magnetosphere as a function of the density ratio, ϵ. The sound speed in the magnetosheath, c_{s2}, is shown as a solid line, the tube speed in the magnetosphere, c_T, is shown as a dotted line, with the slow speed, c_{slow} represented by a dashed line, and the fast speed, c_f, as a dot–dashed line. We have taken $\alpha=0$ in this figure.

$$v_o > \frac{c_f + c_{s2}}{\cos \alpha}, \tag{11}$$

we can see that we would require very large values of the sonic Mach number, v_o in the magnetosheath in order for the modes to become unstable. Indeed, for the trapping of fast body modes we require

$$v_o > \frac{c_f - c_{s2}}{\cos \alpha}, \tag{12}$$

which would still be very high.

III. SLOW MODES

The slow modes are unlikely to be important in the magnetotail since the plasma beta in the tail lobes tends to be very low [typically of the order of 10^{-4}, Saunders (1991)[18]] and so these modes will have very low growth rates. However, we have taken the plasma beta to be of the order of a half throughout this paper in order to properly understand the modes in the magnetotail. The behavior of both the slow body and surface modes is very similar to that in the flank case [Mills *et al.* (1999)[15]] and so we merely summarize the main properties here.

The slow body modes have phase speeds in the range

$$c_T < v_{ph} < c_{\rm slow}, \tag{13}$$

whether they are stable, leaky, or unstable. These modes become unstable when the phase speed crosses the lower cutoff [$v_{ph} = v_o \cos(\alpha) - c_{s2}$] and the growth rates are small and bounded for all values of k and v_o.

The slow surface modes are stable when there is no flow speed and there is a stable mode propagating in the same direction as the flow and one propagating in the opposite direction. As the flow speed the flow speed increases, the phase speed of the modes increases, and these modes coalesce to form one unstable slow surface mode (there is only one since the outgoing boundary condition precludes the other complex solution to the dispersion relation). The phase speed of this unstable mode increases through the range where slow body modes exist [Eq. (13)]. When the phase speed is above the fast speed, the mode restabilizes and splits into two stable fast surface modes. Using the definition of the wave energy that

$$E \propto \omega_r \frac{\partial D}{\partial \omega_r}, \tag{14}$$

where D is the dispersion relation and is defined such that E is positive for any mode when there is no flow in the magnetosheath [see Cairns (1979);[19] Mills *et al.* (1999)[15]], we find that one of these fast surface modes has negative energy and one has positive energy. The positive energy mode has a lower phase speed, and as the flow speed continues to increase, the phase speed tends to the slow speed, $c_{\rm slow}$, and the mode becomes unstable having a small bounded growth rate. The upper, negative energy mode, goes on to coalesce with the positive energy fast surface mode and becomes unstable. This behavior is shown in Fig. 5.

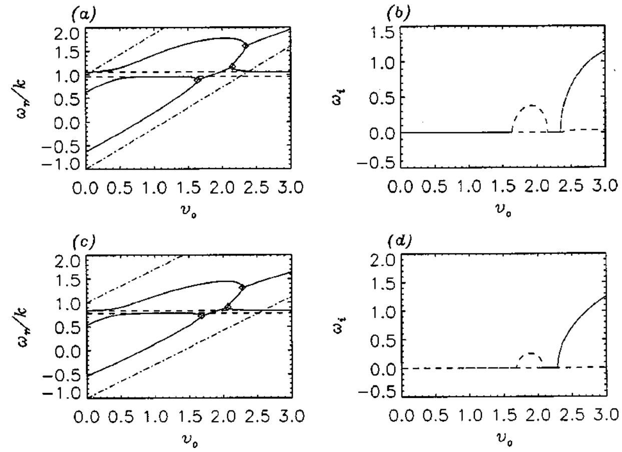

FIG. 5. The phase speeds (a) and (c) and growth rates (b) and (d) of the fundamental slow surface modes as functions of v_o when $k=3$ and $\alpha = \pi/6$ (a) and (b) and $\alpha = \pi/4$ (c) and (d). In each case we have shown both the modes with positive and negative phase speed when $v_o = 0$. We have also shown the fast surface mode which is leaky when $v_o = 0$ in the case $\alpha = \pi/6$ (this occurs when $v_{ph} > v_o \cos \alpha + c_{s2}$, and occurs only very close to $v_o = 0$, with very small growth rates which cannot be seen on this plot). The diamonds mark the points where modes coalesce predicted by the method described in Mills *et al.* (1999) (Ref. 15) and outlined in Sec. IV. The diagonal dot–dashed lines show the upper and lower cut-off speeds, $v_{ph} = v_o \cos \alpha \pm c_{s2}$ and the lower and upper dashed lines show the characteristic phase speeds, c_T and $c_{\rm slow}$, respectively.

The growth rate of the unstable slow surface mode is unbounded in k, however, when β is small, this mode will be unstable only for a very small range of very low v_0 (it is unstable for $c_T + c_{s2} \lesssim v_o \lesssim c_{\rm slow} + c_{s2}$) and is unlikely to be relevant to the magnetotail.

IV. FAST MODES

A. $\alpha \neq 0$

First we investigate the properties of the fast surface and body modes when $\alpha \neq 0$. Figure 6 shows the dependence of the phase speed and growth rate of the fast surface mode on k when $\alpha = \pi/6$ for various values of v_o. When $v_o = 0$ (solid line) the mode is leaky with a small bounded negative growth rate. The mode is stable in the case when $v_o = 2$ and the phase speed is almost constant for all k. As v_o continues

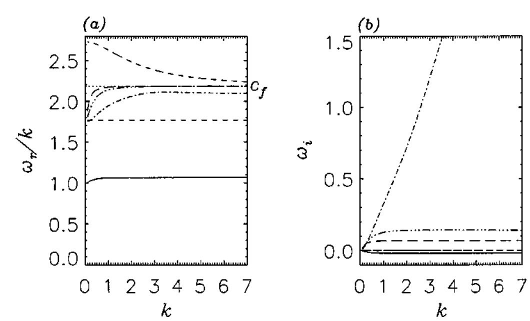

FIG. 6. The dependence of the phase speed (a) and growth rate (b) of the fast surface mode on k when $\alpha = \pi/6$ and $v_o = 0$ (solid line), $v_o = 2$ (lower dashed line), $v_o = 3.25$ (dot–dashed line), $v_o = 6$ (triple dot–dashed line), and $v_o = 10$ (long dashed line). The dotted line indicates the value of the fast speed, c_f, in the magnetosphere. The upper dashed line in (a) shows the phase speed of the stable fundamental fast body mode when $v_o = 2$.

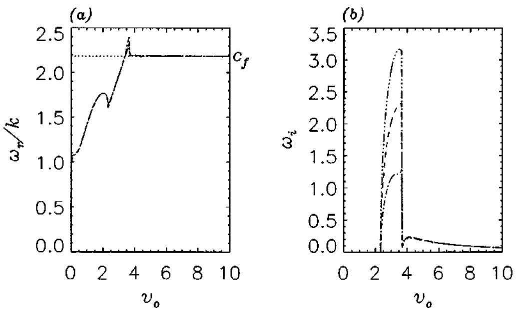

FIG. 7. The dependence of the phase speed (a) and growth rate (b) of the fast surface mode on v_o when $\alpha=\pi/6$ and $k=3$ (dot–dashed line), $k=5$ (dashed line), and $k=7$ (triple dot–dashed line). The dotted line indicates the position of the fast speed, c_f in the magnetosphere.

to increase, having first an unbounded growth rate ($v_o=3.25$—dot–dashed line) and then a bounded one ($v_o=6$, 10, triple dot–dashed line and long dashed line, respectively). When the growth rate becomes bounded, we find that the phase speed tends to c_f as $k\rightarrow\infty$. We have also shown the curve for the stable fundamental fast body mode when $v_o=2$. Note that this mode and the stable fast surface mode may coexist for the same phase speed.

1. Fast surface modes

Figure 7 shows the evolution of the fast surface modes with v_o for various values of the tangential wave number k. The phase speed is almost independent of k for all values of v_o, however, when the mode is first unstable, the growth rate scales linearly with k (so that the growth rate is unbounded), and is then discontinuous at the point at which it becomes bounded in k in Fig. 6, i.e., when $v_o\approx 3.75$.

Now we investigate the onset of instability of these modes for different values of α. Figure 8 is a contour plot of the growth rate of the fast surface mode against v_o and α for $k=10$. We can see that, unlike the flank case, the flow speed at the onset of instability varies very little with angle. In fact, the onset of instability occurs when v_o is close to the Alfvén speed, a result which is in good agreement with Sen (1964)[20] and Ruderman and Wright (1998).[21] The contour plot also shows that the maximum in growth rate for any flow speed occurs when $\alpha\approx\pi/4$. Walker (1981)[22] showed that the maximum growth rate of modes propagating in a system where the field and flow are at an arbitrary angle to one another occurs when the propagation of the modes is close to perpendicular to the direction of the magnetic field—therefore, minimizing the stabilizing effect of magnetic tension. Here, there is no component of the flow perpendicular to the magnetic field and the modes are stable there. Thus the maximum in the growth rate here will occur at an intermediate angle at which the destabilizing effect of the flow dominates over the stabilizing effects of magnetic tension.

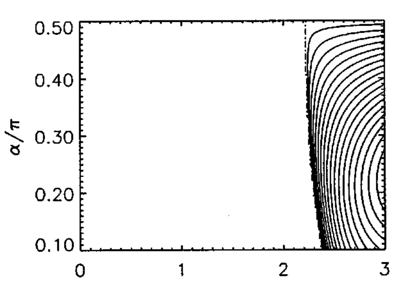

FIG. 8. A contour plot of the growth rate, ω_i, of the fast surface mode against v_o and α. The dot–dashed line shows the onset of instability.

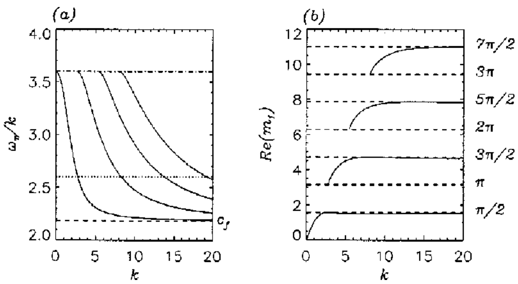

FIG. 9. The dependence of the phase speed (a) and x component of the wave number in the magnetosphere (b) of the stable fast body modes on k when $\alpha=\pi/6$ and $v_o=3$. The dashed line in (a) indicates the value of the fast speed, c_f, in the magnetosphere, while the dot–dashed line shows the upper limit for the existence of stable modes, $v_{ph}=v_o\cos\alpha+c_{s2}$. The dotted line shows $v_{ph}=v_o\cos\alpha$. The dashed lines in (b) indicate integer multiples of $\pi/2$.

2. Fast body modes

In Fig. 9 we show the dispersion diagrams of the fast body modes when they are stable. We have taken $\alpha=\pi/6$ and $v_o=3$ so that

$$\frac{c_f-c_{s2}}{\cos\alpha}<v_o<\frac{c_f+c_{s2}}{\cos\alpha}, \tag{15}$$

is satisfied. In Fig. 9(a) we can see that the phase speed of each mode decreases and tends towards c_f as $k\rightarrow\infty$. In Fig. 9(b) we have plotted the x component of the magnetospheric wave numbers, m_1, for each mode. When the phase speed of a mode is $v_o\cos\alpha+c_{s2}$ the real part of m_1 is an integer multiple of π. This can be seen from the governing equation for stable body modes [Eq. (7)]. At this value of the phase speed, the right hand side of Eq. (7) disappears, so that

$$\tan(m_1)=0, \tag{16}$$

thus, m_1 must be a whole multiple of π. As k increases the phase speed decreases and m_1 increases reaching $m_1=(2n+1)\pi/2$ when $v_{ph}=v_o\cos\alpha$ [shown by a dotted line in Fig. 9(a)], at which point m_1 has a maximum and then decreases slightly before increasing and tending back towards $m_1=(2n+1)\pi/2$ as $v_{ph}\rightarrow c_f$ and $k\rightarrow\infty$. This maximum may be explained by noting that, in the dispersion relation for stable body modes [Eq. (7)],

$$\tan(m_1)\propto\frac{1}{(v_{ph}-v_o\cos\alpha)^2}, \tag{17}$$

so that $\tan(m_1)\rightarrow\infty$ as the phase speed approaches $v_o\cos\alpha$ from both above and below. Therefore, the value of the tan term increases to infinity as the phase speed decreases towards $v_o\cos\alpha$, and then decreases again (remaining posi-

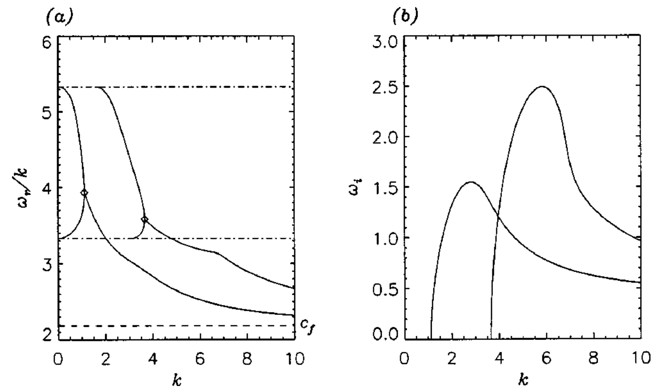

FIG. 10. The dependence of the phase speed (a) and growth rate (b) of the fast body mode harmonics on k when $\alpha=\pi/6$ and $v_o=5$. The dashed line in (a) indicates the position of the fast speed, c_f in the magnetosphere, while the dot–dashed lines shows the upper and lower limits for the existence of stable modes, $v_{ph}=v_o\cos\alpha\pm c_{s2}$.

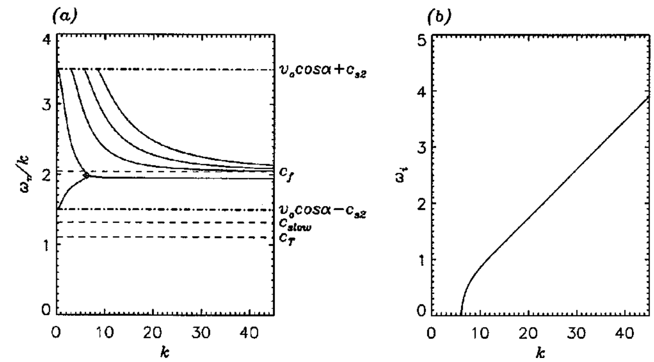

FIG. 11. The dependence of the phase speed (a) and growth rate (b) of the fast body mode harmonics and the fast surface mode on k when $\alpha=0$ and $v_o=2.5$. The dashed lines in (a) indicate the values of the fast speed, c_f, the slow speed, $c_{\rm slow}$, and the tube speed, c_T, in the magnetosphere, while the dot–dashed lines show the upper and lower limits for the existence of stable modes, $v_{ph}=v_o\cos\alpha\pm c_{s2}$. The lower mode for small k in (a) is the negative energy fast surface wave.

tive) as the phase speed continues to decrease. Thus m_1 increases to $m_1=(2n+1)\pi/2$ and then decreases as the phase speed continues to decrease.

Figure 10 shows the phase speed and growth rate of the first two harmonics when $v_o=5$ and $\alpha=\pi/6$ (so that $v_o\cos\alpha>c_f+c_{s2}$) in which case the modes are unstable. As for the flank case studied by Mills *et al.* (1999)[15] we find that there are two stable fast body modes for each harmonic, a positive and a negative energy wave and that the onset of the instability occurs when these two modes coalesce. The diamonds in Fig. 10(a) shows the point where the coalescence of the modes is predicted to occur by the method detailed in Mills *et al.* (1999).[15] This is done by finding double roots of the dispersion relation (roots such that the dispersion relation is satisfied and the derivative of the dispersion relation with respect to the phase speed, v_{ph}, is also zero). The growth rates of these modes once they are unstable are bounded in this case. However, as with the flanks case there will always be one fast mode which has unbounded growth rate and has a dominantly surface mode character.

B. $\alpha=0$

We now consider the dispersion of the fast surface and body modes when the propagation of the modes is parallel to both the magnetospheric magnetic field and the flow in the magnetosheath.

Figure 11 shows the dispersion of the fast modes when $v_o=2.5$ and $\alpha=0$, i.e.,

$$v_o\cos\alpha-c_{s2}<c_f<v_o\cos\alpha+c_{s2}, \tag{18}$$

and we would expect the fast body modes to be stable for all k. The second, third, and fourth body mode harmonics are indeed stable for all k and have $v_{ph}\to c_f$ as $k\to\infty$. However, the phase speed of the fundamental body mode decreases through c_f (the mode remains stable through this transition) and coalesces with the fast surface mode, becoming unstable. This fast surface mode is the one with negative energy formed when the slow surface mode restabilizes. This behavior is totally different to that found for these modes when $\alpha\neq0$ (shown in Fig. 9). Once the two modes have coalesced, the growth rate is unbounded as k increases, but the phase speed remains constant below the fast speed. The point where the two modes coalesce may be predicted using the same method as that for the case when $\alpha\neq0$.

Figure 12 shows the real (solid lines) and imaginary (dot–dashed lines) parts of the x component of the wave number in the magnetosphere for the modes shown in Fig. 11. The dashed lines indicate integer multiples of $\pi/2$. For the higher harmonics, the wave number is $n\pi$ when the phase speed is v_o+c_{s2}. As k increases, the phase speed decreases and m_1 increases reaching a maximum when $v_{ph}=v_o$. At this point, the right-hand side of Eq. (7) becomes infinitely large so that $m_1=(2n-1)\pi/2$. Then, increasing k further, the phase speed continues to decrease approaching c_f. Now the wave numbers tend back towards $m_1=n\pi$. Again, this is different to the $\alpha\neq0$ case where $m_1\to(2n-1)\pi/2$ for large k. The reasons for these discrepancies in behavior will be explained in Sec. IV C. The following properties of m_1 can be seen from Eq. (7): The wave number of the fundamental mode is zero when $k=0$ and ω_r/k is finite.

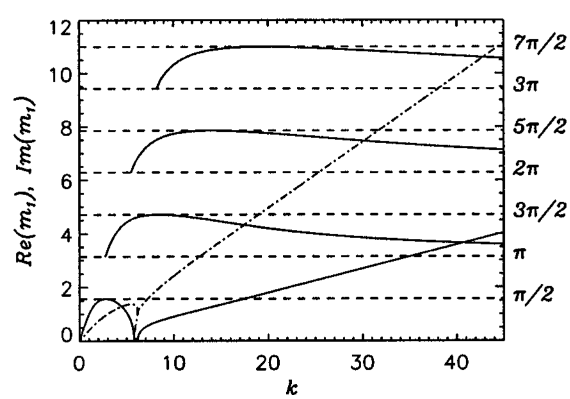

FIG. 12. The dependence of the x component of the wave number in the magnetosphere, m_1, on k when $v_o=2.5$ and $\alpha=0$. The solid lines show the real parts of the wave number and the dot–dashed lines show the imaginary parts. The dashed lines show integer multiples of $\pi/2$. The dot–dashed line for low k corresponds to the negative energy fast surface wave shown in Fig. 11.

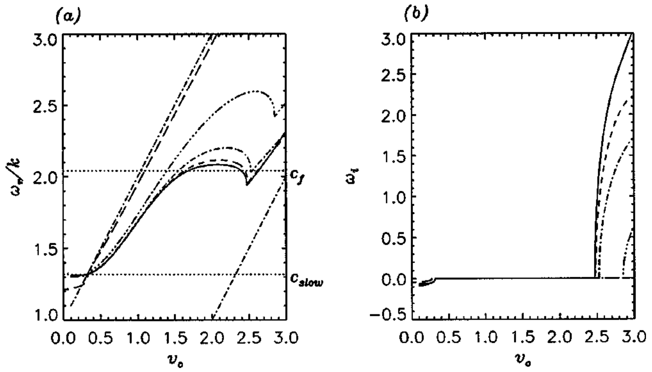

FIG. 13. The dependence of the phase speed (a) and growth rate (b) of the fundamental fast body mode harmonics/the fast surface mode on v_o when $\alpha=0$ and $k=10$ (solid line), $k=7.5$ (dashed line), $k=5$ (dot–dashed line), $k=2.5$ (triple dot–dashed line), and $k=0.5$ (long dashed line). The dotted lines in (a) indicates the fast speed, c_f, and the slow speed, c_{slow}, in the magnetosphere, while the diagonal dot–dashed lines shows the upper and lower limits for the existence of stable modes, $v_{ph}=v_o \cos\alpha \pm c_{s2}$.

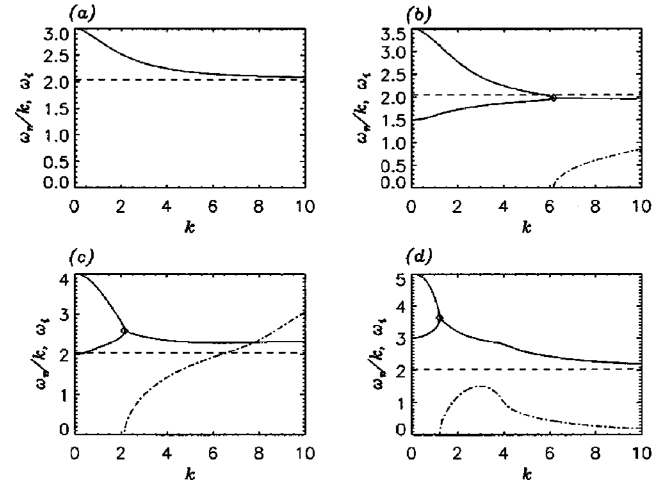

FIG. 14. The phase speed (solid lines) and growth rate (dot–dashed lines) of the fundamental fast mode and the negative energy wave (where applicable) as functions of k when $\alpha=0$ and (a) $v_o=2$, (b) $v_o=2.5$, (c) $v_o=3$, and (d) $v_o=4$. The dashed lines show the value of the fast speed, c_f.

It then increases as k increases reaching a maximum when $v_{ph}=v_o$ and $m_1=\pi/2$. As the phase speed of the mode decreases through c_f, the numerator of Eq. (3) vanishes and the real part of the wave number decreases to zero. The imaginary part of the wave number becomes nonzero when $v_{ph}<c_f$, i.e., the mode becomes a fast surface mode. As k increases further the positive and negative energy fast surface modes coalesce and become unstable, and at this point the wave number becomes complex.

In Fig. 13 we see the variation of the behavior of this fast mode with v_o for various values of k. For all values of k the mode is a leaky fast surface mode for low v_o, and becomes a stable fast surface mode when $v_o=c_{\mathrm{slow}}-c_{s2}$ (which is the first speed at which m_2 may be purely imaginary for phase speeds for which the mode is a fast surface mode). The phase speed of the mode then increases as v_0 increases and crosses the line $v_{ph}=c_f$. At this point the mode becomes a stable fundamental body mode [which has m_1 purely real, see Eq. (3)]. The phase speed increases to a maximum, with the maxima occurring at larger values of v_{ph} for smaller values of k (since the phase speed of a fast body mode decreases as k increases) and then decreases to the point at which the instability begins. For $k=10$ (solid line) and $k=7.5$ (dashed line) the onset of instability occurs when the phase speed is below the fast speed. Therefore, for these values of k, the mode becomes a stable fast surface mode again just before the onset of the instability. For lower values of k, the onset of instability occurs for phase speeds above the fast speed, so that the mode remains a stable fast body mode up to the point at which the instability begins. This mode is the upper (coalescing) mode shown in Fig. 11(a) the lower mode comes from the restabilization of the unstable slow surface mode into a fast surface mode as discussed in Sec. III and is a negative energy wave. The transition of the fast surface mode into a fast body mode occurs for lower flow speeds as k decreases, and as $k\to 0$, the point of transition occurs when

$$v_o=c_f-c_{s2}. \tag{19}$$

It is interesting to note that in this case, the positive energy fast surface mode and the fundamental fast body mode cannot coexist. Indeed, for any flow speed and given k, only one of these modes may exist and in analysing the change in these modes with a change in flow speed, we find that the phase speed of the mode may cross the line $v_{ph}=c_f$ continuously as m_1 vanishes. Roberts (1981)[23] studied the dispersion of field aligned modes in a slab model without flow and found only either fast body modes or fast surface modes for any set of parameters (see Fig. 1 of that paper). When $\alpha \neq 0$ the stable fast surface mode and fundamental body mode may both exist for some values of v_o. The reasons for this discrepancy are explained in Sec. IV C.

Figure 14 shows the phase speed (solid lines) and growth rate (dot–dashed lines) of this mode as functions of k for various values of v_o. In Fig. 14(a) we have taken $v_o=2$ and here the mode is a stable fast body mode for all k, with $v_{ph}\to c_f^+$ as $k\to\infty$. The slow surface mode has not restabilized to become a fast surface mode yet for this flow speed and so this mode is not plotted here. In Fig. 14(b) we have increased the flow speed to $v_o=2.5$ (which is the case shown in Fig. 11) we see that the upper mode is a fast body mode for small k, becoming a fast surface mode just before becoming unstable as k increases. The lower mode in this figure is the negative energy fast surface mode. When $v_0=3$ [in Fig. 14(c)], the negative energy mode has phase speed just below the fast speed when $k\to 0$ so that it is a fast surface mode here. As k increases, the mode becomes a fast body mode, coalescing with the upper mode to become unstable. When $v_o=2.5$, the mode is dominantly a surface mode as $k\to\infty$, however, when $v_o=3$, the real part of m_1 grows faster than the imaginary part. Finally, in Fig. 14(d), the flow speed is increased to $v_o=4$, and the modes are both fast body modes for small k. For large k, the growth rate is bounded.

Finally, we look at the behavior of a fast body mode with negative phase speed (corresponding to a mode propagating earthwards in the magnetotail). Figure 15 shows the

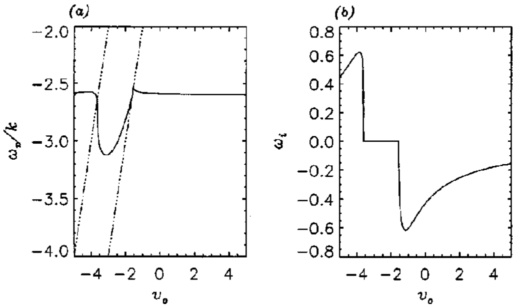

FIG. 15. The dependence of the phase speed (a) and growth rate (b) of the second fast body mode harmonic on v_o when $\alpha=0$ and $k=5$. The diagonal dot–dashed lines shows the upper and lower limits for the existence of stable modes, $v_{ph}=v_o\cos\alpha\pm c_{s2}$.

phase speed and growth rate of the second harmonic fast body mode as functions of the flow speed in the magnetosheath. Modes with negative phase speed are stable when the phase speed satisfies the same inequalities as for positive phase speed [Eq. (10)]. In this case we find the mode is unstable for large negative flow speeds, becomes stable while the flow speed is still negative, and as the flow speed increases, the mode becomes leaky. This is different to the modes with positive phase speed which are leaky for low (or negative flow speeds) and unstable for high flow speeds. Thus we would expect modes propagating towards the earth in the magnetotail to be leaky. However, we find that the decay rate, ω_i, approaches zero as the flow speed increases, so that the modes will not loose energy very quickly as they propagate towards the earth if v_o is sufficiently large.

C. Explaining the difference between $\alpha\neq 0$ and $\alpha=0$

The dispersion relation for stable fast body modes is

$$\tan(m_1)=\frac{\epsilon}{c_{s2}}\frac{(v_{ph}^2-v_{a1}^2\cos^2\alpha)}{(v_{ph}-v_o\cos\alpha)^2}\sqrt{\frac{(c_{s2}^2-(v_{ph}-v_o\cos\alpha)^2)(c_f^2+c_{\text{slow}}^2)(v_{ph}^2-c_T^2)}{(v_{ph}^2-c_f^2)(v_{ph}^2-c_{\text{slow}}^2)}},\tag{20}$$

while that for stable fast surface modes is

$$\tanh(n_1)=\frac{\epsilon}{c_{s2}}\frac{(v_{ph}^2-v_{a1}^2\cos^2\alpha)}{(v_{ph}-v_o\cos\alpha)^2}\sqrt{\frac{(c_{s2}^2-(v_{ph}-v_o\cos\alpha)^2)(c_f^2+c_{\text{slow}}^2)(v_{ph}^2-c_T^2)}{(c_f^2-v_{ph}^2)(v_{ph}^2-c_{\text{slow}}^2)}},\tag{21}$$

where m_1 is the wave number in the x direction in the magnetosphere and $n_1=im_1$. Examining this equation we find different behaviors in the two cases (i) $\alpha\neq 0$, and (ii) $\alpha=0$. Taking the first case and letting $v_{ph}\to c_f$ on the right-hand side of Eqs. (20) and (21) we find that

$$|\tan(m_1)|\to\infty \quad\text{and}\quad |\tanh(n_1)|\to\infty,\tag{22}$$

respectively. Therefore, when $v_{ph}\to c_f^+$ (body modes)

$$m_1\to\frac{(2n+1)\pi}{2}.\tag{23}$$

However, when $v_{ph}\to c_f^-$ (surface modes) there are no real values of n_1 which satisfy the equation, and thus there may be no stable surface modes with phase speeds close to c_f.

Conversely, when $\alpha=0$, $c_f=v_{a1}$ and the dispersion relation for stable body modes reduces to

$$\tan(m_1)=\epsilon\frac{\sqrt{(v_{ph}^2-v_{a1}^2)(c_{s2}^2-(v_{ph}-v_o\cos\alpha)^2)}}{c_{s2}(v_{ph}-v_o\cos\alpha)^2}\times\sqrt{\frac{(c_f^2+c_{\text{slow}}^2)(v_{ph}^2-c_T^2)}{(v_{ph}^2-c_{\text{slow}}^2)}},\tag{24}$$

and the equation for fast surface modes reduces to

$$\tanh(n_1)=\epsilon\frac{\sqrt{(v_{a1}^2-v_{ph}^2)(c_{s2}^2-(v_{ph}-v_o\cos\alpha)^2)}}{c_{s2}(v_{ph}-v_o\cos\alpha)^2}\times\sqrt{\frac{(c_f^2+c_{\text{slow}}^2)(v_{ph}^2-c_T^2)}{(v_{ph}^2-c_{\text{slow}}^2)}}.\tag{25}$$

Thus when $v_{ph}\to c_f^+$, $\tan(m_1)\to 0$ so that

$$m_1\to n\pi,\tag{26}$$

and when $v_{ph}\to c_f^-$, $\tanh(n_1)\to 0$ and, therefore,

$$m_1\to 0.\tag{27}$$

In other words, both stable body and surface modes may have phase speeds close to the fast speed in this case. This explains how, in this case, the character of the fast modes may change smoothly between having an oscillatory and an evanescent character in the magnetosphere. We can see this transition in Fig. 11(a) when the phase speed of the fundamental fast cavity mode decreases to below c_f while the mode is still stable (therefore, changing from a body to a surface mode). In Fig. 14(c) we see the phase speed of the fast surface mode increasing through c_f, so in this case the mode changes from a fast surface mode to a fast body mode.

V. DISCUSSIONS AND CONCLUSIONS

We have investigated the trapping and excitation of fast modes in the magnetotail. We have found that the speed at which fast surface modes first become unstable varies little with the direction in which the modes are propagating. This is in agreement with the results found by Pu and Kivelson (1983).[11] However, we did not find the upper cutoff speed reported by Pu and Kivelson.[11] This is because the bounded magnetotail does not allow the energy released by the instability to be carried away from the boundary to infinity. For our equilibrium the maximum growth rate of these modes is found to occur at an angle of about $\pi/4$. This is due to the stabilizing force of the magnetic tension and the destabilizing effect of the flow varying with angle. Walker (1981)[22] found that the most unstable modes propagate at angles close to perpendicular to the magnetic field. In our model, the flow has no component perpendicular to the magnetic field, so the maximum growth rate will occur at some intermediate position.

Fast body modes may first become unstable when $v_o \cos\alpha = c_f + c_{s2}$, so that modes propagating parallel to the flow and magnetic field will become unstable first. We found that the behavior of both the fast surface mode and the fast body mode is different for modes propagating parallel to the magnetic field than for those propagating perpendicular to it. Only one of the stable fundamental fast body mode and the stable fast surface mode (having positive energy) may exist for any given flow speed when $\alpha = 0$, and the phase speeds of these modes may change continuously across $v_{ph} = c_f$. When $\alpha \neq 0$, these modes are separate and the phase speed of the fast surface mode may not approach the fast speed.

We take the width of the magnetotail to be 25 R_E and the sound speed in the magnetosheath as 100 km/s. Although we have used a density ratio of 0.192 in our calculations, this was merely for convenience so we could calculate the qualitative behavior of the modes without needing to have overly high flow speeds. A more realistic value of the density ratio would be 0.02, corresponding to an Alfvén speed of about 700 km/s. With typical magnetosheath flow speeds of 500 km/s, and the onset of instability for the fast surface modes being close to the Alfvén speed, we can see that the fast magnetopause surface mode is unlikely to be KH unstable in this region. Ruderman and Wright (1998)[21] discussed this behavior and showed that below the critical speed for the KH instability (KHI), negative energy surface waves may propagate on the magnetopause. These may drive Alfvén resonances within the magnetotail and when this occurs the surface mode becomes unstable and both the surface mode and the resonance grow. Therefore, any unstable modes observed on the magnetopause are likely to be caused by this resonant interaction between negative energy waves and Alfvén waves rather than directly by the KHI.

Fast body modes propagating away from the Earth may become unstable when $v_o > c_f + c_{s2}$, corresponding to a speed of 800 km/s, and they are trapped when $c_f - c_{s2} < v_o < c_f + c_{s2}$, corresponding to a speed of 600–800 km/s in dimensional units. Thus, these modes will become trapped only at times of high solar wind flow.

We have also found negative energy waves, although we do not drive any Alfvén resonances as our magnetotail is taken to be uniform and the velocity shear is a vortex sheet. We have shown that these unstable modes correspond to modes which propagate in a positive direction in the rest frame of the magnetosheath, but in a negative direction in the magnetospheric rest frame. The onset of instability occurs at the coalescence of positive and negative energy waves.

Observations of oscillations in the magnetotail show that fast modes may be excited down tail and propagate earthward [Elphinstone *et al.* (1995)[12]]. Models of this have tended to treat the magnetopause as a perfectly reflecting boundary trapping these modes within the magnetotail [e.g., Allan and Wright (1998);[13] Wright (1994)[24]]. An important consequence of our model is that we may better understand the nature of the interaction of these modes with the magnetopause. We have shown that modes propagating towards the Earth in the magnetotail (i.e., those modes which have negative phase speeds) are leaky for positive flow speeds. In fact, the modes are leaky for any flow speed that satisfies $v_o > c_{s2} - c_f$, or in dimensional units $v_o > -600$ km/s, so they will certainly be leaky for any realistic flow speed. However, the growth rate (or in this case, the decay rate) of each mode becomes very small as the flow speed increases. Therefore, we expect the modes to be essentially stable and for the majority of the wave energy to be reflected from the magnetopause. We conclude, therefore, that the assumption of a reflecting magnetopause in the wave guide models is a reasonable approximation.

The dimensional frequency of the fast wave guide modes in our model is about 4 mHz which is of the same order of magnitude as those observed [e.g., by Herron (1967)[8]].

Overall we have found that the magnetotail will be stable to the Kelvin–Helmholtz instability for most values of the flow speed in the magnetosheath. However, both earthward and tailward propagating fast body modes will be leaky with small decay rates, and will lose only a small amount of energy as they reflect from the magnetopause, so that treating the magnetosphere in this region as a perfect reflector is a reasonable approximation and waveguide models should be successful in predicting the behavior of these modes.

If surface or waveguide modes are observed to be unstable in the magnetotail, this could point to the occurance of a resonant instability [Ruderman and Wright (1998)] operating, and is an important calculation for future research.

ACKNOWLEDGMENTS

K. J. M. was supported by a PPARC Research Studentship and A. N. W. was supported by a PPARC Advanced Fellowship.

[1] J. W. Dungey, Phys. Rev. Lett. **6**, 47 (1961).
[2] J. W. Dungey, J. Geophys. Res. **70**, 1753 (1965).
[3] T. J. Herron, J. Geophys. Res. **72**, 759 (1967).
[4] J. F. McClay and H. R. Radoski, J. Geophys. Res. **72**, 4525 (1967).
[5] G. L. Siscoe, J. Geophys. Res. **74**, 6482 (1969).
[6] J. F. McKenzie, J. Geophys. Res. **75**, 5331 (1970).
[7] W. Seboldt, J. Geophys. Res. **95**, 10471 (1990).
[8] W. W. Liu, B. L. Xu, J. C. Samson, and G. Rostoker, J. Geophys. Res. **100**, 79 (1995).
[9] P. M. Edwin, B. Roberts, and W. J. Hughes, Geophys. Res. Lett. **13**, 373 (1986).
[10] J. M. Smith, B. Roberts, and R. Oliver, Astron. Astrophys. **327**, 377 (1997).
[11] Z. Y. Pu and M. G. Kivelson, J. Geophys. Res. **88**, 841 (1983).

[12] R. D. Elphinstone, D. J. Hearn, L. L. Cogger, J. S. Murphree, A. Wright, I. Sandahl, S. Ohtani, P. T. Newell, D. M. Klumpar, M. Shapshak, K. Mursula, T. A. Potemra, and J. A. Sauvaud, J. Geophys. Res. **100**, 12093 (1995).
[13] W. Allan and A. N. Wright, J. Geophys. Res. **103**, 2359 (1998).
[14] J. F. McKenzie, Planet. Space Sci. **18**, 1 (1970).
[15] K. J. Mills, A. N. Wright, and I. R. Mann, Phys. Plasmas **6**, 4070 (1999).
[16] K. J. Mills and A. N. Wright, J. Geophys. Res. **104**, 22667 (1999).
[17] I. R. Mann, A. N. Wright, K. J. Mills, and V. M. Nakariakov, J. Geophys. Res. **104**, 333 (1999).
[18] M. Saunders, in *Advances in Solar System Magnetohydrodynamics*, edited by E. R. Priest and A. W. Hood (Cambridge University Press, Cambridge, 1991).
[19] R. A. Cairns, J. Fluid Mech. **8**, 1 (1979).
[20] A. K. Sen, Phys. Fluids **7**, 1293 (1964).
[21] M. S. Rudermann and A. N. Wright, J. Geophys. Res. **103**, 15697 (1998).
[22] A. D. M. Walker, Planet. Space Sci. **29**, 293 (1981).
[23] B. Roberts, Sol. Phys. **69**, 39 (1981).
[24] A. N. Wright, J. Geophys. Res. **99**, 159 (1994).